InnoVationinfo

Journal of
Biomedical Research and Reviews

ISSN: 2581-7388

Volume 6: 1

J Biomed Res Rev 2023

Introducing a Novel *in-vitro* Model of Thrombolysis in Acute Ischemic Stroke

Anushree Dwivedi[1]

John Burke[2]

Mahmood Mirza[1]

Michael Gilvarry[1]

Ray McCarthy[1*]

[1]*Cerenovus (Johnson & Johnson), Galway Neuro Technology Centre, Galway, Ireland*

[2]*Departmnet of Biomedical Engineering, National University of Ireland Galway, Galway, Ireland*

Abstract

Thrombolytic treatment of Acute Ischemic Stroke (AIS) patients with recombinant tissue plasminogen activator (r-tPA) may not restore flow in the occluded vessel. Thrombolysis is a complex process involving a biochemical process of clot lysis but it is also occurring in a physically dynamic environment that involves mechanical stresses on the clot. Numerous studies using in-vitro models have been carried out to understand the mechanism of thrombolysis. However, the focus of these *in-vitro* models has been largely on biochemical fibrinolysis and not on hydromechanical forces. *In vivo* studies using animals and clinical studies in humans incorporate both biochemical and hydromechanical effects, however they don't allow for direct visualization of the clot breakdown during thrombolysis, making it difficult to separately study both modes of action. Having an *in-vitro* model that gives a clear visualization of the process may help to better understand the hydromechanical component of thrombolysis. To achieve this visualization, we set out to develop an *in-vitro* model that can be used to observe the mechanical break-down of clot analogues during lysis by r-tPA by simulating physiological flow and pressure conditions in a transparent model of the M1 segment of the middle cerebral artery. In our experiments conducted in a constrained vessel, RBC rich clots and fibrin rich clots showed no significant difference in clot size after thrombolysis. However, in a compliant vessel, RBC rich clots were found to experience faster reduction in clot size in comparison to the fibrin rich clots. RBC rich clots were observed to have a wider range of movement under pulsed flow than fibrin rich clots resulting in a more rapid reduction in clot size through clot fragmentation. These findings may prove beneficial in understanding the treatment effect of thrombolysis for different AIS patients.

Keywords: Acute ischemic stroke, Thrombolysis, *in-vitro* models.

Introduction

Large vessel occlusions (LVOs) in Acute Ischemic Stroke (AIS) are one of the major causes of disability and mortality globally. The medical recanalization route involves treating patients with recombinant-tissue plasminogen activator (r-tPA) referred to as intravenous thrombolysis (IVT). The mechanism of action involves r-tPA attaching to fibrin on the surface of the clot. Consequently, fibrin bound plasminogen is changed to its active form, plasmin, which cleaves fibrin. Cleavage of the fibrin

Article Information

Article Type: Research Article

Article Number: JBRR-166

Received Date: 13 February, 2023

Accepted Date: 28 March, 2023

Published Date: 04 April, 2023

***Corresponding author:** McCarthy R, Department of Biomedical Engineering, National University of Ireland Galway, Block 3, Ballybrit Business Park, Galway, Co. Galway, Ireland.

Citation: Dwivedi A, Burke J, Mirza M, Gilvarry M, McCarthy R (2023) Introducing a Novel *in-vitro* Model of Thrombolysis in Acute Ischemic Stroke. J Biomed Res Rev Vol: 6, Issu: 1. (01-11).

mesh eventually leads to degradation of thrombus and recanalization of the occluded blood vessel. The rate of successful LVO recanalization in AIS patients is still low for IVT treatment, but outcomes for these patients have been improved greatly with the introduction of the complimentary therapy of mechanical thrombectomy (MT) [1-3]. For patients that undergo fibrinolysis followed by MT, structural changes of partially lysed clots may affect subsequent endovascular treatment by mechanical thrombectomy (MT) [4,5]. Adverse effects of thrombolysis include increased risk of haemorrhage, while partial clot lysis can cause thrombus migration or fragmentation which may still occlude distal arteries [6,7]. To identify advantages and disadvantages of thrombus migration following thrombolysis, an in-depth evaluation of changes in thrombus characteristics is required [5,8-10].

An animal study in rats using different imaging techniques has shown changes in clot location during thrombolysis resulting in downstream clot displacement [11]. In addition to this, it has been shown that poor collaterals inhibited the effect of thrombolysis resulting in poor outcomes [12,13]. Friction, shear stress and compression may act on the clot in an occluded vessel, potentially leading to clot movement or fragmentation, which may be determined by the mechanical properties of the clot itself [14-16]. Structural, shape and mechanical changes occurring in clots due to fibrinolysis are largely unknown and have not been represented very well in the existing *in-vitro* studies [17-21]. Due to the gaps in *in-vitro* modelling and lack of experimental data, accurate translation to numerical studies has been a challenge [22].

Clinical studies have shown that thrombolytic therapy changes the biochemical composition over time [23]. Characteristics such as clot size and red blood cell (RBC) content have been shown to influence responsiveness to r-tPA [24,25]. Evaluation of the effect of thrombolysis in an animal model has highlighted clot composition as a critical factor affecting the rate of re-perfusion, which was attributed to different mechanical and molecular changes occurring during clot preparation [26]. *In vitro* tests have confirmed that administration of r-tPA significantly affects clot mechanical properties [27]. We hypothesized that direct visualization of in-vitro thrombolysis experiments would enhance our understanding of how these changes manifest in LVO treatment.

Using clots with different cellular composition, we developed an *in-vitro* model of thrombolysis that incorporates the physical parameters of blood flow and pressure in an LVO. The model allowed visualization of occlusion dynamics during the time of lysis. In this way it was observed that differences in clot physical behaviour during r-tPA treatment are associated with recanalization rate, which may help to understand treatment effects for AIS patients.

Materials and Methods

R-tPA treatment of LVO's of the middle cerebral artery (MCA) were conducted using two artery models, to investigate the effect of thrombolysis on different types of clots. One model was made from compliant silicone and the other from rigid glass. These vessel models were incorporated in a flow system that circulated ovine serum in a loop. R-tPA was infused for over one hour using the recommended dose. Ovine clots were prepared with 10-20% red blood cell (RBC) and 60%-80% RBC composition to develop fibrin rich and RBC rich clots, respectively. Changes in the vessel occlusions were measured visually and using pressure and flow sensors.

Blood clot preparation

Ovine blood was obtained from Ash Stream Ltd, Co. Mayo, Ireland in a sterile blood bag pre-loaded with anti-coagulant solution ACPD (adenine citrate phosphate dextrose). Whole blood was spun in a centrifuge at 2200g to separately collect plasma and red blood cells (RBC). Clots were prepared by varying the RBC content and plasma in the blood mixture to create blood clots of desired RBC composition using previously reported methods [28]. To develop RBC rich clots (60-80% RBC approximately by histology), a 30% RBC blood mixture was used and for preparing fibrin rich clots (10-20% RBC approximately by histology), a 5 % RBC blood mixture was utilized. The clot analogues were stored under controlled temperature conditions and allowed to mature overnight. Serum from clots prepared from the same sheep was collected and stored at -20^{o} C for use during thrombolysis.

Flow model

An *in-vitro* flow system was set up with inlet and outlet reservoirs placed at different heights to generate a flow, and to achieve controlled pressure conditions in the model. Serum flowed from a primary header tank, which was placed at a height of 130 cm to generate mean arterial pressures (MAP) of approximately 110 mm Hg, which acted on the proximal face of the occlusion. A secondary header tank set at a lower height above the occlusion model was used to generate pressure on the distal face of the occlusion. High- and low-pressure gradients across the clots of 70 +/- 10 mm Hg and 10 +/-2 mm Hg were achieved by adjusting the height of the secondary header tank to 40 cm or 90 cm, respectively. These pressure gradients span the range of clinical measurements in AIS patients as described by Sorimachi et al [29]. In this study, the pressure proximal, and distal of the occlusions was 95+/13.2 mm Hg and 35.9 +/- 13.5mm Hg respectively.

The schematic flow model is shown in figure 1. Pulsed flow was achieved using a modified peristaltic pump attached proximally to the occluded vessel via a branch from the main flow loop, which terminated in a close-ended compliant tube of 8.5 mm internal diameter and 150 mm length. Pulsatile flow was achieved by removing one roller from the 2-roller pump-head, which allowed a pulsed reflux of the fluid drawn from the main flow loop. The pulse generator is based on a design from Desjardins et al [30]. The total volume of the system was 350 ml approximately. The two interchangeable vessel models made from silicone and glass were alternatively attached to the flow system, which were referred as the "test vessel" and "control vessel", respectively. Clot analogues

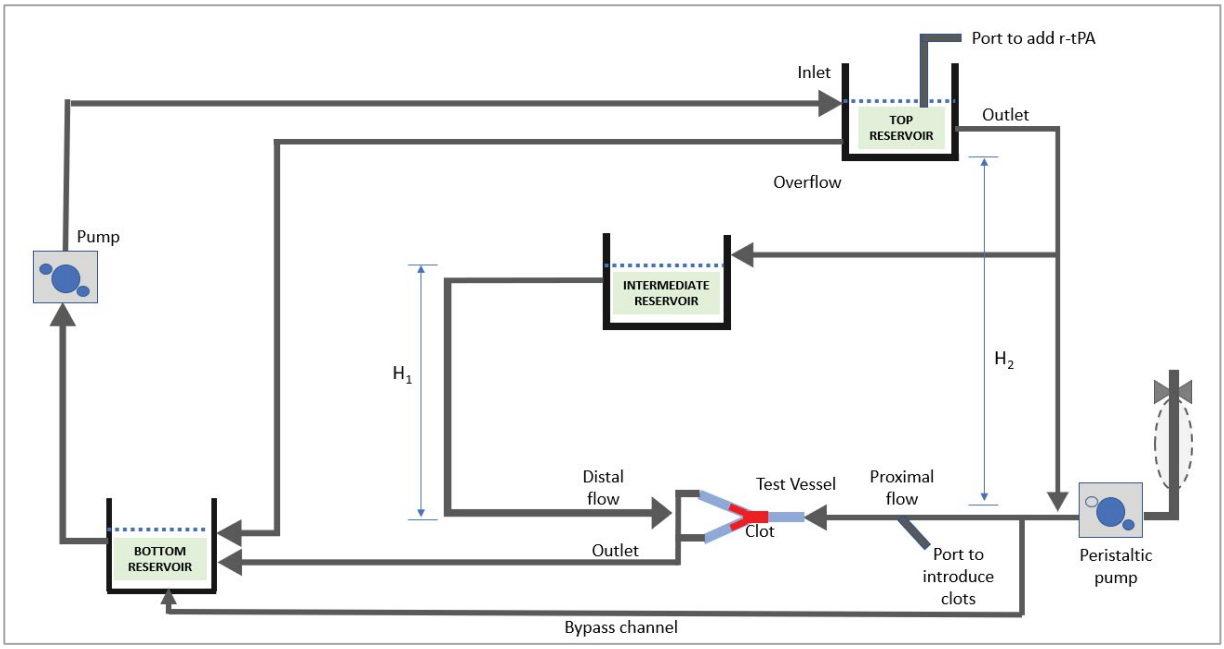

Figure 1: Schematic of the thrombolysis flow model showing flow paths in the system incorporating pulsatile flow.

were allowed to flow into the vessels and lodged at the same location every time. A flow meter was attached to the distal vessels beyond the occlusion along with pressure sensors, whilst a proximal pressure sensor was also used to monitor antegrade pressure. Movement of the clot was captured using a camera.

The *test vessel* comprised of a compliant silicone bifurcated vessel which was manufactured using silicone with 13% compliance for a change in 100 mm Hg (BDC Laboratories, Colorado, USA). The vessel consists of a main trunk with 3.5 mm internal diameter (ID) (representing the M1 segment of the MCA) that bifurcates to 2 vessels with 2.5 mm ID tapered to 2.0 mm ID over a length of 70 mm (Figure 2 A,B). Recanalization was achieved when full flow was restored in either of the branches of the test vessel. The experiment was halted after full recanalization of a branch was achieved. Two timepoints were identified to describe the speed of recanalization, (i) the starting point of recanalization, when any flow was detected in a distal vessel, and (ii) the time when full recanalization was achieved, when flow through a distal branch reached its pre-occlusion flow rate. Orthogonal confirmation of these timepoints was achieved by observation of simultaneous pressure increase recorded in the distal pressure sensors.

The *control vessel* model is a tapered glass vessel, designed to prevent clot migration and to enable continuous flow to both the proximal and distal faces of the occlusion. The gradual taper combined with a focal restriction at the distal end of the vessel act to prevent distal migration of the clot, while still allowing diffusion or flow through the occlusion if possible. Additionally, flow to the proximal and distal faces of a clot could be adjusted so that either continuous flow or stagnant flow conditions could be replicated (Figure 3 C,D).

r-tPA infusion and dosing

A concentration of 1mg/ml of rt-PA (Alteplase, Boehringer Ingelheim) was prepared by reconstituting 50 mg of the Alteplase lyophilized powder with 50 ml of sterile water. Alteplase was infused over time after administration of a 10% initial bolus to achieve the equivalent of a 0.9 mg/kg dose, which equates to a concentration of 14 µg/ml in the serum.

Pre-conditioning of clots

To understand the changes in the clot analogues due to compression under fluid pressure, clot analogues were placed in a mock vessel without thrombolysis. In this evaluation, RBC rich and fibrin rich clots were exposed to pulsatile flow under blood pressure for a duration of three hours. Clots were observed for movement and change in size periodically over this time. Furthermore, it was assessed if the compression of clot in a constrained vessel under blood pressure alters the response to thrombolysis. Thrombolysis of clots was performed in a test tube on a compacted clot removed from the flow model after 1 hour and a non-compacted clot that was not introduced to the flow model.

Flow model experimental method

For all experiments, clots were lodged in the vessels prior to adding rt-PA for one hour under continuous flow conditions and constant pulsatile pressure to allow clot compaction to reach a stable level. All test conditions are provided in the table 1. r-tPA was administered to the primary reservoir and from there it could circulate through the full flow model. Each experiment was carried out in triplicate. In the test vessel, both a high-pressure gradient and a low-pressure gradient were evaluated at 70+/-10 mm Hg and 10+/-2 mm Hg, respectively. In the control vessel all experiments were carried out at a pressure gradient of 10

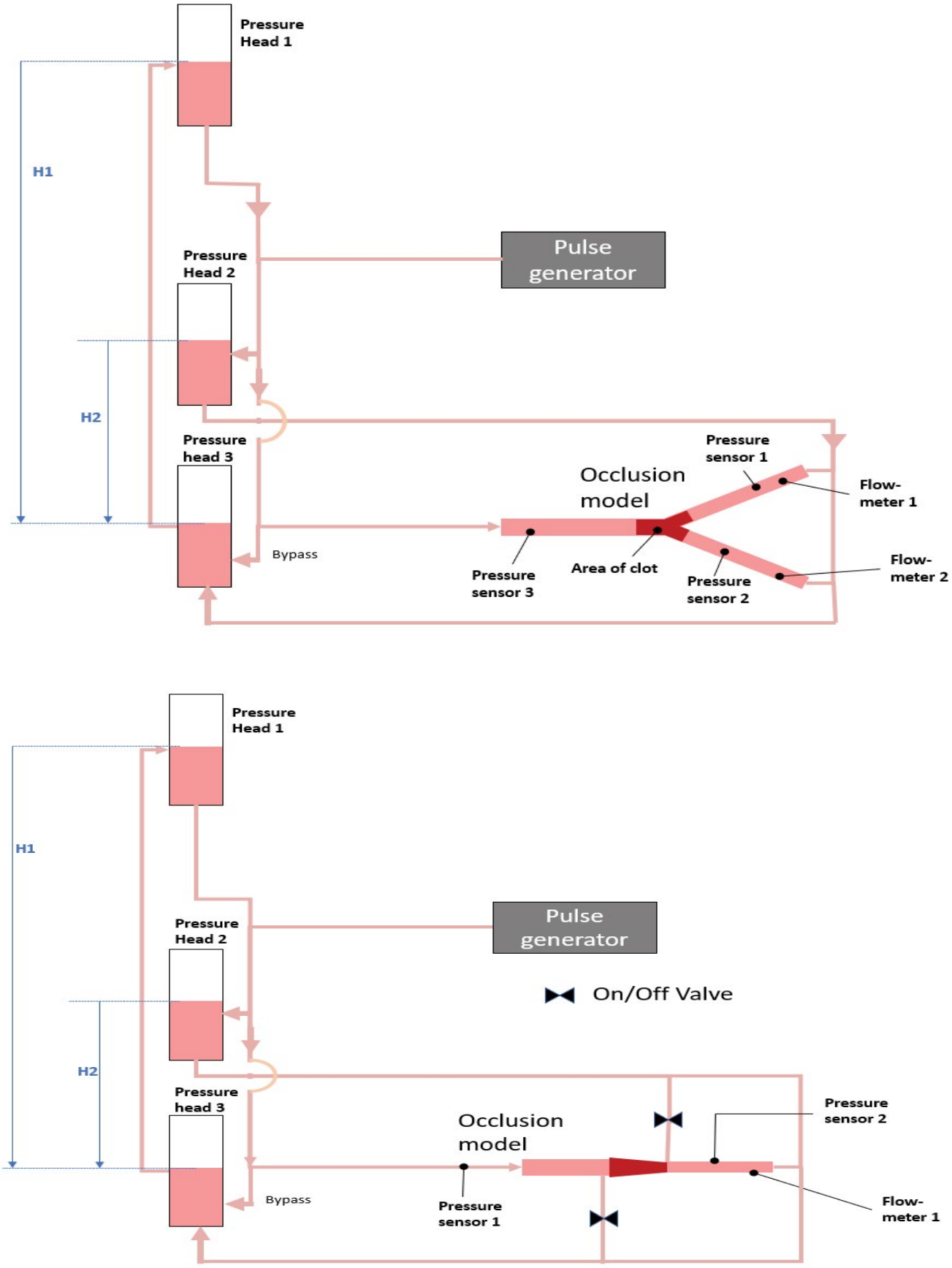

Figure 2: (A) schematic of the test vessel integrated with the flow model. **(B)** Image of clot analogue occluding the test vessel; **(C)** Simplified schematic of the test (non-compliant tapered glass) vessel depicting an occlusion in the M1 vessel of MCA. **(D)** Image of a clot analogue occluding the control vessel. H1 and H2 are heights determining proximal and distal pressure in the occlusion model.

Test Condition	Vessel	Clot	Pressure drop (mm Hg)	Duration of test	Nearest branch to proximal face of clot	Nearest branch to distal face of clot	Starting clot length (mm)	Replicates
1	Test	RBC Rich	70	Until full flow restored in the vessel	2-3 mm	60 mm	12 mm	3
2	Test	RBC Poor	70	Until full flow restored in the vessel	2-3 mm	60 mm	12 mm	3
3	Test	RBC Poor	10	Until full flow restored in the vessel	2-3 mm	60 mm	12 mm	3
4	Control	RBC Poor	10	2 hr	0 mm	0 mm	18 mm	3
5	Control	RBC Rich	10	2 hr	0 mm	0 mm	18 mm	3
6	Control	RBC Rich	10	2 hr	30 mm	60 mm	18 mm	3
7	Control	RBC Rich	10	2 hr	10 mm	0 mm	8 mm	3
8	Control	RBC Poor	10	2 hr	10 mm	0 mm	8 mm	3
9	Test tube	RBC Rich (No pre-compaction)	Not-applicable	1 hr	NA (No r-tPA treatment)	NA (No r-tPA treatment)	18 mm	5
10	Test tube	RBC Poor (No pre-compaction)	Not-applicable (NA)	1 hr	NA (No r-tPA treatment)	NA (No r-tPA treatment)	18 mm	5
11	Test tube	RBC Rich (No pre-compaction)	Not-applicable (NA)	1 hr	NA (Fully immersed in r-tPA)	NA (Fully immersed in r-tPA)	18 mm	5
12	Test tube	RBC Rich (Pre-compacted in control vessel)	10 (Pre-compaction)	1 hr	NA (Fully immersed in r-tPA)	NA (Fully immersed in r-tPA)	18 mm	5

Table 1: Test conditions; Starting clot length: Indicates length of the clot in the occluded vessel.

+/-2 mm Hg. The effect of changing the clot size was also evaluated in the control vessel.

Changes in pressure were recorded in real time proximal and distal to the clot and flow rate was also monitored using a flow meter. Mean arterial pressure (MAP) was recorded proximal and distal to the clot in both branches of the *test vessel* which were referred as left or right branches. Pulse pressure (PP), which is the difference between the maximum and the minimum pressure was also recorded proximally and distally to the clot. To investigate the effect of r-tPA on clot size reduction, images of the clots were recorded at different intervals for the duration of 2 hours; change in clot area was calculated by analysing the images using ImageJ software (version 1.53J 2021).

Statistical analysis

All data are presented as mean ± standard deviation. A two-sample t-test was used to examine significant differences between two variables or a one-way ANOVA with Bonferroni test was used if more than 2 variables were compared. Differences were considered significant at $p < 0.05$. Statistical analyses were performed using Graph Pad Prism 8 or Minitab (version 17.3.1).

Results

Pre-conditioning of clot before undergoing thrombolysis

During the pre-conditioning of the clots before undergoing thrombolysis, it was observed that clots reduced in size due to compaction within the first hour after lodgement but did not reduce in size after one hour. Therefore, clot samples were allowed to lodge for an hour under the desired pressure conditions in the flow model before thrombolysis treatment (Supplementary figure 1A). An average reduction of 3.7 +/- 1.75 % (N=5) and 8.9 +/- 5.38 % (N=5) in clot size was observed in RBC rich and fibrin rich clots respectively in one-hour duration.

Thrombolysis performed in a test tube on a compressed and a non-compressed clot revealed that compression of clot in a constrained vessel under blood pressure slowed down thrombolysis of the clots when subsequently placed in a test tube containing r-tPA. Clots that were not placed in the flow model underwent a significantly greater reduction in mass during thrombolysis as compared with clots that had undergone compression in the flow-model (49.5 +/- 7.5 % vs. 31.9 +/- 7.9 %; Mean +/- SD; N=5; p=0.007) (Supplementary figure 1B).

Thrombolysis of clots in the flow model

Flowrate readings obtained in the test vessel at regular intervals distal to the occlusion showed that vessels with RBC rich clots re-established full flow through the occluded vessel faster in comparison to fibrin rich clots (Figure 3A).

During thrombolysis at a pressure gradient of 70 mmHg across the clot, it took an average of 15.6 minutes for RBC rich occlusions and 44.3 minutes (average, N=3) for fibrin rich occlusions to fully recanalize the vessel after onset of vessel opening. after onset of vessel opening (Table 2). Occlusions involving fibrin rich clots with a 10 mm Hg pressure gradient across the clot, took a slightly faster time of 36.3 minutes (average, N=3). Pressure measurements obtained proximal and distal of the clots are shown in figure 3B. The pressure curves showed a similar pattern to the that of the flow rate measurements. Controls with no r-tPA treatment shown in

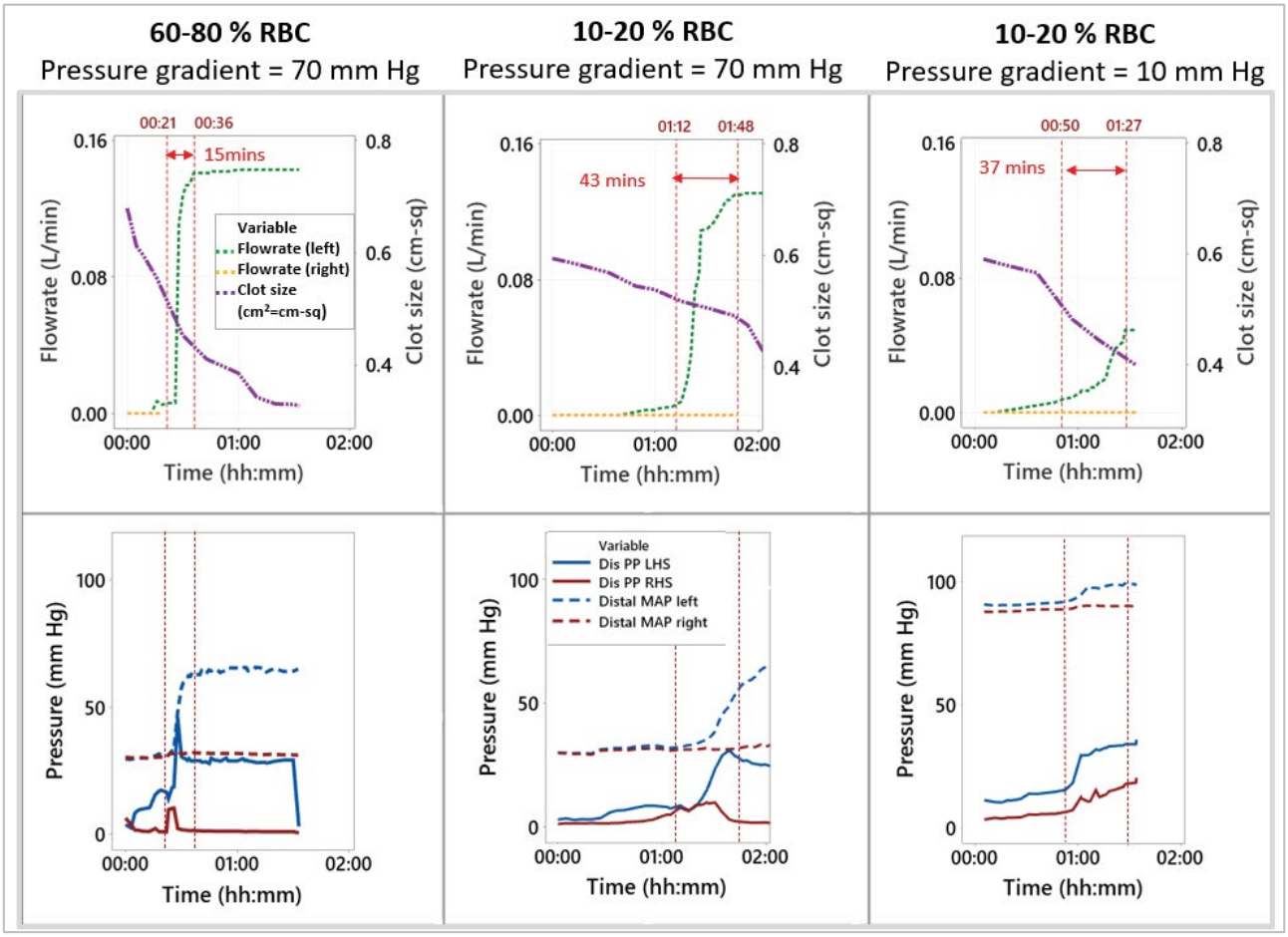

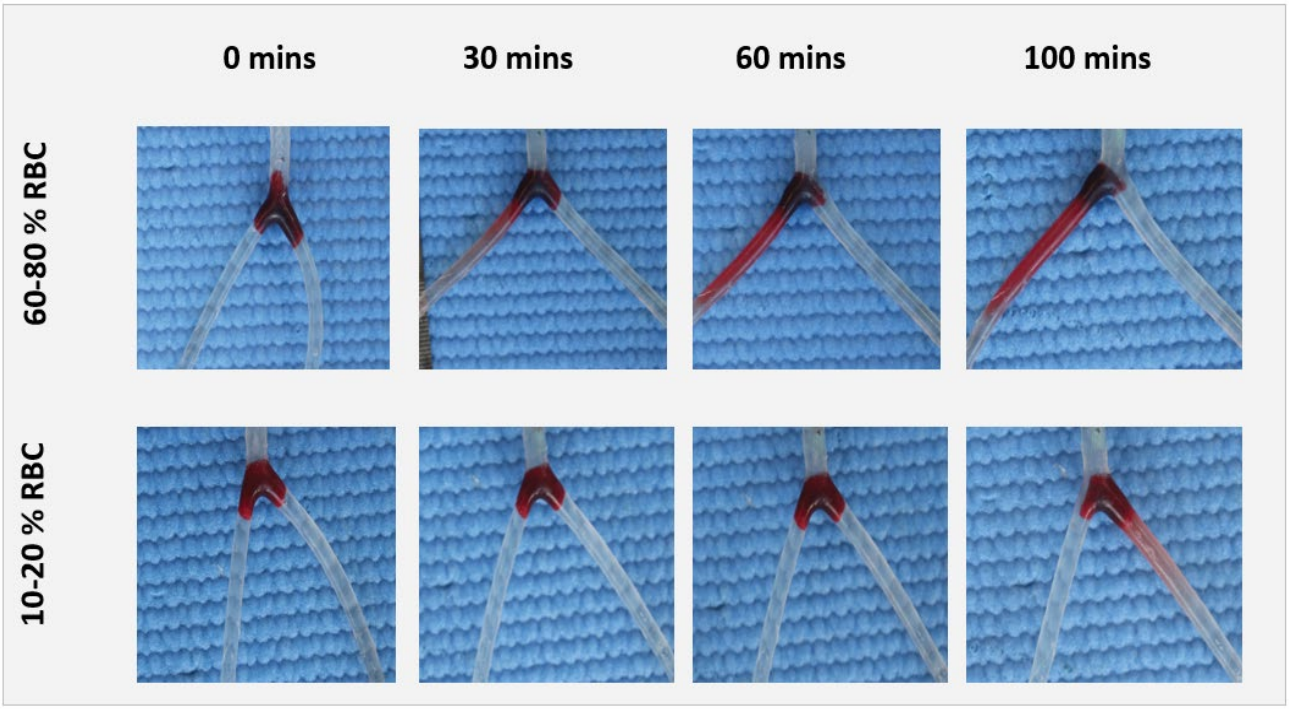

Figure 3: (A) Representative graphs showing real time lysis profiles of a typical fibrin rich (10-20% RBC content) and RBC rich clots (60-80% RBC content), RBC rich clots attained 50% through a branch of the vessel faster than fibrin rich clots, N=3; The first red dotted line denotes start of recanalization, then the next grey line depicts time when 50% flow was restored in a branch of the vessel and the last red line denoted time when full recanalization occurred in the vessel. LHS= Left hand side; PP= Pulse pressure; RHS= Right hand side, MAP = Mean Arterial Pressure. **(B)** Representative graph showing lysis profiles of a typical fibrin rich (10-20% RBC content) and RBC rich clot (60-80% RBC content) depicting changes in pressure proximal and distal to the clot during thrombolysis; Centimetre square (cm^2) = cm-sq. **(C)** Representative images of an RBC and fibrin rich clot getting lysed over a period of time, showing reduction in clot size at high pressure gradient.

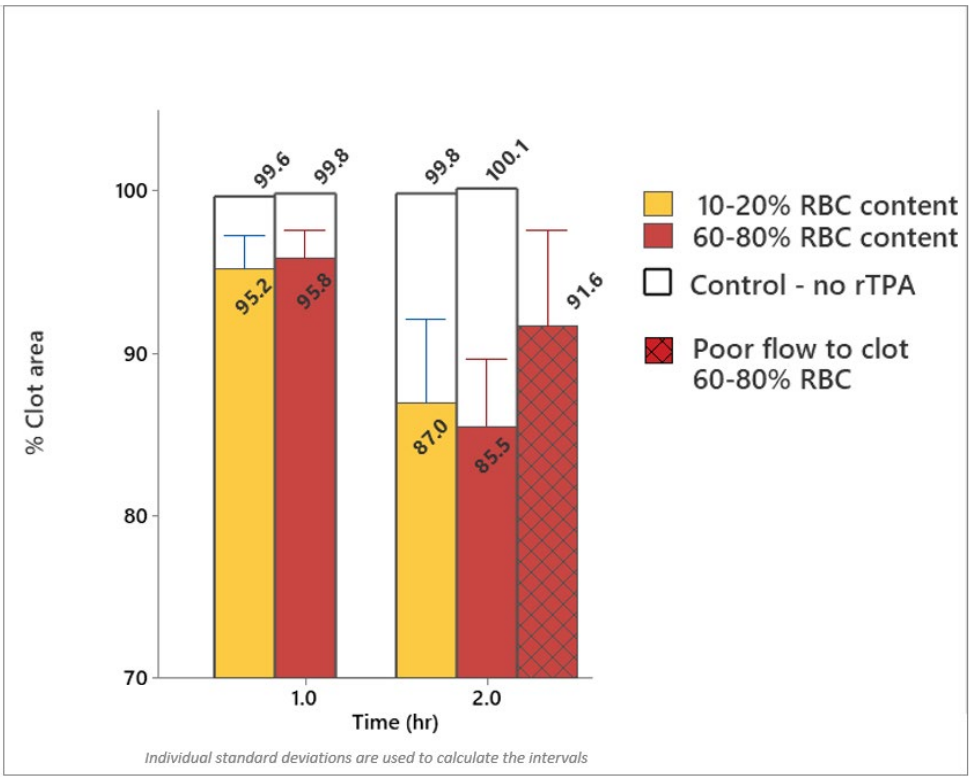

Figure 4: Graph showing minimal changes in clot size between RBC rich and fibrin rich clots at high pressure gradient. Small changes were observed in RBC rich clots with flow and poor flow up to the face of the clot in the glass vessel model. Please note data was combined here for long and short clots as no difference was observed in clot size between these conditions during thrombolysis (N >=6).

Test condition	Clot type and pressure gradient (mm Hg)	T_{RS} (mins)	dT (T_{RS}– T_{END}) (mins)	Reduction in clot size before any opening (Ts -T_{RS}) (%)	Reduction in clot size after initial opening (T_{RS}-T_{END}) (%)	Reduction in clot size overall (T_S-T_{END}) (%)
1	RBC rich 70	21, 47,86 **[51.3]**	15, 10, 22 **[15.6]**	10.5, 6.5, 24.8 **[14.0]**	29.2, 20.3 15.3 **[21.6]**	39.7, 26.8, 40.1 **[35.5]**
2	RBC poor 70	43, 53,72 **[56.0]**	43, 55, 35 **[44.3]**	2.8, 5.1, 9.4 **[5.76]**	20.1, 10.4, 9.9 **[13.5]**	22.9, 15.5, 19.3 **[19.3]**
3	RBC poor 10	50, 28, 87 **[55.0]**	37, 29, 41 **[35.7]**	4.3, 0.81, 1.73 **[2.26]**	28.2, 30.0, 21.0 **[26.4]**	32.5, 30.8, 22.7 **[27.6]**
4	RBC poor 10	No recanalization, Experiment stopped at 120 mins				10.3, 6.1, 10.0 **[8.8]**
5	RBC rich 10					**11.8** +/- 4.8; N=6
6	RBC rich 10(poor flow)					12.3, 5.4, 7.4 **[8.4]**
7	RBC rich 10(short clot)					15.6, 12.4, 29.6 **[19.2]**
8	RBC poor 10(short clot)					14.8, 17.3, 21.7 **[17.9]**
9	RBC rich (No pre-compaction)	No Recanalization, Experiment stopped at 60 mins				**3.7** +/- 1.7; N=5
10	RBC poor (No pre-compaction)					**8.9** +/- 5.4; N=5
11	RBC rich (Non-compacted)					**49.5** +/- 7.5; N=5
12	RBC rich (Compacted)					**31.9** +/- 7.9; N=5

T_S = Starting time point of the experiment; T_{RS} = Time for beginning of recanalization (mins); T_{End} = Time to achieve full recanalization through a vessel or end of experiment if no recanalization was achieved. **dT** = (T_{RS}– T_{END})

Table 2: Depicting time period required by different clot types to achieve flow restoration in the test vessel. Average of the individual values has been shown in the brackets [ ] +/- depicts standard deviation. Time here depicts time since start of the thrombolysis experiment in minutes. NA (Not applicable)

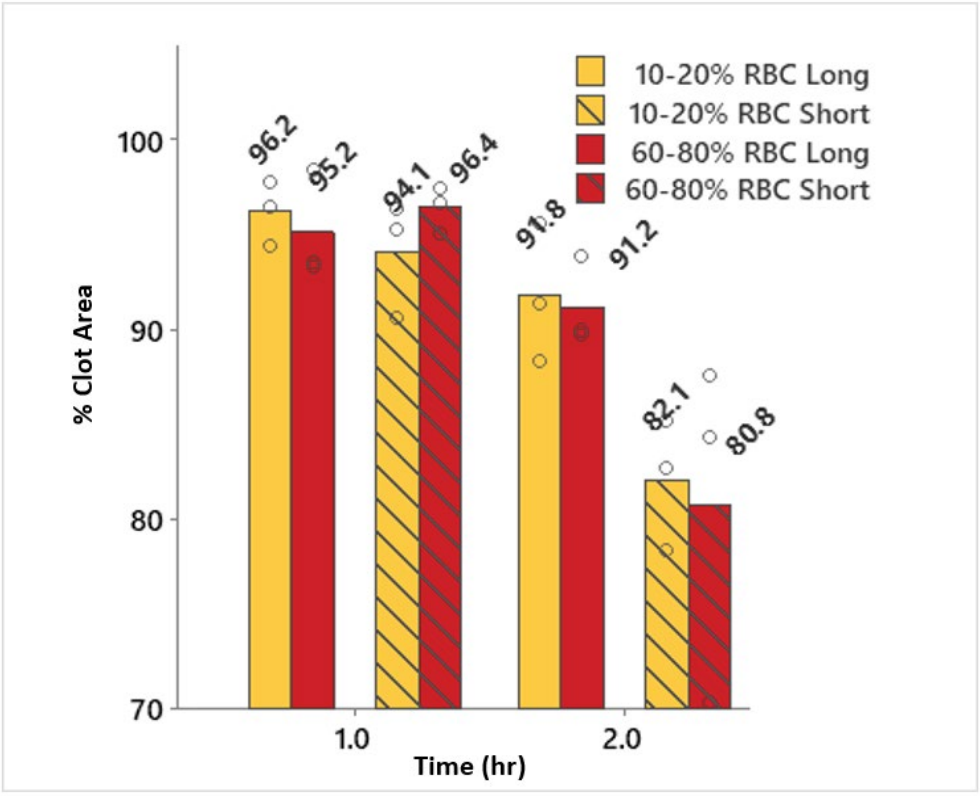

Figure 5: Graph showing minimal changes in clot size between RBC rich and fibrin rich clots.

Supplementary figure 3, did not recanalize at all in the same time period.

Significant pulsatile movement of the RBC rich clots was visible in the vessel while fibrin rich clots moved minimally, which is captured in supplementary video 1. RBC rich clots also shed clot fragments once a channel opened through the occlusion as shown in supplementary video 2, which was not observed with fibrin rich clots. In the test vessel, fibrin rich clots displayed an average of 7.97% reduction in clot size while RBC rich clots displayed average of 25.36 % reduction in clot size 60 minutes after addition of r-tPA (N=3). A representative image of the clots has been shown in Figure 3C and corresponding table highlights average reduction in clot size (N=3).

The control vessel was used to study the effect that clot composition has on the rate of lysis when clot movement is restricted. None of these evaluations resulted in the restoration of flow in the occluded vessel even after 2 hours. Minimal reduction in the size of the clots was observed and there was no significant impact on the rate of lysis due to the RBC content of the clots. Fibrin rich and RBC rich clots showed a similar reduction of 4.4 % and 4.0 % after 1 hour and 12.8 % and 14.5 % after 2 hours respectively (Average N =6). Comparing stagnant flow to good flow to the clot faces in RBC rich clots, they reduced in size by 8.4 % for the former in comparison to 14.5 % for the latter (average N=3) (Figure 4).

Fibrin rich and RBC rich clots with different lengths (occupying the full 18mm vessel length or only 8 mm vessel length) showed 8.2% and 8.8% reduction in clot size after 2 hours, respectively. Whereas the short length fibrin rich and RBC rich clots showed 17.9% and 19.2% reduction in clot size (Figure 5). However, loss in clot size for each clot type was similar, with 0.047 cm^2 and 0.045 cm^2 for the large and short length RBC rich clots and 0.044 cm^2 and 0.058 cm^2 (Average, N=3) for the large and short length fibrin rich clots after r-tPA treatment; thus indicating that the mode of clot attrition is likely caused by erosion of material from the clot faces rather than through diffuse fibrinolysis throughout the clots.

Discussion

Models of thrombolysis that have been developed mostly include in-vitro models, microfluidic models, and computational numerical models [20,31-36]. However, they all lack the ability to combine the biochemical factors with the mechanical factors of realistic thrombi, pressure, flow, vessel compliance, and general blood flow conditions [20,31]. In numerical studies, assumptions were needed to reduce complexity, such as ignoring the intrinsic pathway of thrombolysis, clot fragmentation ability during lysis, migration of clots after fragmentation, pulsatility and vessel compliance [36-39]. Furthermore, there is a lack of sufficient experimental data to validate the numerical models of thrombolysis, and the experimental studies generally don't correspond well to physiological mechanisms *in-vivo* [22].

To overcome these challenges, we developed an *in-vitro* model with different types of vessel compliance and vessel design to help explain the mechanism of clot lysis. In

previous work we confirmed that r-tPA has similar efficacy on human and ovine blood clots in an in-vitro setting [27]. In this present study, we observed that the compaction of clot slowed down clot lysis, which suggests that compression reduced permeability of r-tPA into the clot structure. This is congruent to other studies that showed a compacted clot structure with reduced pores increased resistance to clot lysis [40-42]. In our *in-vitro* model setup consisting of a compliant bifurcated vessel, recanalization was achieved quicker with RBC rich clots in comparison to fibrin rich clots. As expected, when recanalization occurred, flow rate increase was matched by pressure equalization in the recanalized vessel. It has been well reported that RBC rich clots are more susceptible to thrombolytics than fibrin rich clots, possibly due to microstructural differences. In our model, as the occluded vessels started to recanalize, this was preceded by observation of a pulse pressure registering in the distal vessel, indicating some movement of the clot as it started degrading. RBC rich clots in our experiment moved more and visibly fragmented during thrombolysis, creating a sharper rate of recanalization than fibrin rich clots which didn't move as much and didn't break apart into visible fragments. Mechanistically, this may be explained by studies that showed RBC rich clots are more prone to fracture [14,43].

We believe, increased fragmentation of RBC rich clots can also be attributed to more rapid clot movement facilitated by differences in the mechanical properties' clots with different clot composition. Clot composition dependant properties such as friction coefficient, stiffness and fracture toughness, have been reported [15,44]. We propose that reduced stiffness and lower friction coefficient in RBC clots result in more movement, which may lead to higher fatigue. In addition to this, RBC rich clots have lower fracture toughness, also resulting in greater fatigue in a pulsed flow. Combining all these factors, suggests that RBC rich clot occlusions open up faster than similar sized Fibrin rich clots when treated with r-tPA.

In order to separate the influence of clot movement and direct r-tPA access, the compliant test vessel was swapped with a non-compliant glass vessel model (control vessel) that kept the clot in one place while giving r-tPA access in a controlled manner to both the proximal and distal face of the clot. This test showed no difference in clot degradation of RBC rich clots compared to fibrin rich clots. Suggesting clot material was removed from the faces (proximal and distal) of both clot types in a layer by layer fashion, as suggested by other studies. An interesting study highlighted that when r-tPA is introduced at the edge of the clot, lysis occurs spatially advancing from the front of the clot over time, restricting the amount of r-tPA available to the deep sections of the clots [45-47].

This study had several limitations. The number of replicates for each condition in these experiments were low (N=3) due to limited blood that could be collected from an animal at a time. This study was performed in an *in-vitro* flow model which limits the direct applicability to *in vivo* animal and human studies. Human blood clots were not used for all the experiments due to limited availability of human blood and easier working conditions with animal (specifically ovine) blood. However, we have previously shown ovine blood clots to behave similarly to human blood clots in a thrombolysis model. Despite these limitations, this study represents a foundation for translating thrombolysis findings to *in-vivo* studies. The *in-vivo* clot vessel interaction and extracellular matrix could not be created in this *in-vitro* model which might have implications on thrombolysis. Homogenous clots prepared for this study do not clinically represent thrombi retrieved from AIS patients but for the purpose of this study these clot analogues enabled us to carry out repeatable testing and compare results.

Further investigations to fully elucidate the effect of r-tPA on clots would prove beneficial for physicians in making treatment decisions for AIS patients [48]. These findings should be considered to evaluate thrombus dynamics in a clinical trial for achieving acute reperfusion. This work may also provide outputs to support computational model generation of thrombolysis treatment as part of the in-silico trials [14,49-52].

Conclusion

We successfully developed an *in-vitro* model of LVO thrombolysis that replicate *in-vivo* physiological conditions. Using these models, we identified the importance of thrombus composition on the speed of LVO recanalization, which may explain some of the clinical observations related to clot composition and thrombolysis efficacy. RBC rich clots oscillated more under pulsed pressure than fibrin rich clots. The lower stiffness and friction coefficient result in more movement of RBC clots, which may lead to higher clot fatigue during the fibrinolysis process. Once a channel opens through the occluded vessel, there is significant shearing of the clot, resulting in more fragmentation of RBC rich clots. Clot mechanical properties, which are closely linked to their histological composition may have a large role in the efficacy of IVT. This novel thrombolysis model may have utility in evaluating the efficacy of different thrombolysis treatments in the in-vitro setting.

Funding

This project has received funding from the European Union's Horizon 2020 research and innovation program under grant agreement no. 777072.

Acknowledgment

Would like to thank all the INSIST project investigators.

References

1. Bhatia R, Hill MD, Shobha N, Menon B, Bal S, et al. (2010) Low rates of acute recanalization with intravenous recombinant tissue plasminogen activator in ischemic stroke: Real-world experience and a call for action. Stroke 41: 2254-2258.

2. Menon BK, Al-Ajlan FS, Najm M, Puig J, Castellanos M, et al. (2018) Association of clinical, imaging, and thrombus characteristics with recanalization of visible intracranial occlusion in patients with acute ischemic stroke. JAMA 320: 1017-1026.

3. Seners P, Turc G, Maïer B, Mas JL, Oppenheim C, et al. (2016) Incidence and Predictors of Early Recanalization after Intravenous Thrombolysis:

A Systematic Review and Meta-Analysis. Stroke 47: 2409-2412.

4. Kaesmacher J, Giarrusso M, Zibold F, Mosimann PJ, Dobrocky T, et al. (2018) Rates and Quality of Preinterventional Reperfusion in Patients With Direct Access to Endovascular Treatment. Stroke 49: 1924-1932.

5. Kaesmacher J, Maegerlein C, Kaesmacher M, Zimmer C, Poppert H, et al. (2017) Thrombus Migration in the Middle Cerebral Artery: Incidence, Imaging Signs, and Impact on Success of Endovascular Thrombectomy. Journal of the American Heart Association 6.

6. Alves HC, Treurniet KM, Jansen IGH, Yoo AJ, Dutra BG, et al. (2019) Thrombus Migration Paradox in Patients With Acute Ischemic Stroke. Stroke 50: 3156-163.

7. Ren Y, Churilov L, Mitchell P, Dowling R, Bush S, et al. (2018) Clot migration is associated with intravenous thrombolysis in the setting of acute ischemic stroke. Stroke 49: 3060-3062.

8. Kim YD, Nam HS, Kim SH, Kim EY, Song D, et al. (2015) Time-Dependent Thrombus Resolution after Tissue-Type Plasminogen Activator in Patients with Stroke and Mice. Stroke 46: 1877-1882.

9. Mueller L, Pult F, Meisterernst J, Heldner MR, Mono ML, et al. (2017) Impact of intravenous thrombolysis on recanalization rates in patients with stroke treated with bridging therapy. European Journal of Neurology 24: 1016-1021.

10. Ohara T, Menon BK, Al-Ajlan FS, Horn M, Najm M, et al. (2021) Thrombus Migration and Fragmentation After Intravenous Alteplase Treatment. Stroke 52: 203-212.

11. Busch E, Krüger K, Allegrini PR, Kerskens CM, Gyngell ML, et al. (1998) Reperfusion after thrombolytic therapy of embolic stroke in the rat: magnetic resonance and biochemical imaging. Journal of cerebral blood flow and metabolism 18: 407-418.

12. Angermaier A, Langner S, Kirsch M, Kessler C, Hosten N, et al. (2011) CT-angiographic collateralization predicts final infarct volume after intra-arterial thrombolysis for acute anterior circulation ischemic stroke. Cerebrovascular diseases 31: 177-184.

13. Wufuer A, Wubuli A, Mijiti P, Zhou J, Tuerxun S, et al. (2018) Impact of collateral circulation status on favorable outcomes in thrombolysis treatment: A systematic review and meta-analysis. Experimental and Therapeutic Medicine 15: 707.

14. Fereidoonnezhad B, Dwivedi A, Johnson S, McCarthy R, McGarry P (2021) Blood clot fracture properties are dependent on red blood cell and fibrin content. Acta Biomaterialia 127: 213-228.

15. Gunning GM, McArdle K, Mirza M, Duffy S, Gilvarry M, et al. (2018) Clot friction variation with fibrin content; implications for resistance to thrombectomy. Journal of NeuroInterventional Surgery 10: 34-38.

16. Johnson S, McCarthy R, Gilvarry M, McHugh PE, McGarry JP (2021) Investigating the Mechanical Behavior of Clot Analogues Through Experimental and Computational Analysis. Annals of Biomedical Engineering 49: 420-431.

17. Greenberg RK, Ouriel K, Srivastava S, Shortell C, Ivancev K, et al. (2000) Mechanical versus chemical thrombolysis: an in vitro differentiation of thrombolytic mechanisms. Journal of vascular and interventional radiology 11: 199-205.

18. Komorowicz E, Kolev K, Léránt I, Machovich R (1998) Flow rate-modulated dissolution of fibrin with clot-embedded and circulating proteases. Circulation research 82: 1102-1108.

19. Nikitin D, Choi S, Mican J, Toul M, Ryu WS, et al. (2021) Development and Testing of Thrombolytics in Stroke. Journal of Stroke 23: 12-36.

20. Prasad S, Kashyap RS, Deopujari JY, Purohit HJ, Taori GM, et al. (2006) Development of an in vitro model to study clot lysis activity of thrombolytic drugs. Thrombosis Journal 4: 14.

21. Stief TW (2006) In vitro simulation of therapeutic thrombolysis with microtiter plate clot-lysis assay. Clinical and applied thrombosis/hemostasis : official journal of the International Academy of Clinical and Applied Thrombosis/Hemostasis 12: 21-32.

22. Petkantchin R, Padmos R, Boudjeltia KZ, Raynaud F, Chopard B (2022) Thrombolysis: Observations and numerical models. Journal of Biomechanics 132: 110902.

23. Czaplicki C, Albadawi H, Partovi S, Gandhi RT, Quencer K, et al. (2017) Can thrombus age guide thrombolytic therapy? Cardiovascular Diagnosis and Therapy 7(Suppl 3): S186-S196.

24. Bilgic AB, Gocmen R, Arsava EM, Topcuoglu MA (2020) The Effect of Clot Volume and Permeability on Response to Intravenous Tissue Plasminogen Activator in Acute Ischemic Stroke. Journal of stroke and cerebrovascular diseases : the official journal of National Stroke Association 29: 104541.

25. Choi MH, Park GH, Lee JS, Lee SE, Lee SJ, et al. (2018) Erythrocyte fraction within retrieved thrombi contributes to thrombolytic response in acute ischemic stroke. Stroke 49: 652-659.

26. Niessen F, Hilger T, Hoehn M, Hossmann KA (2003) Differences in clot preparation determine outcome of recombinant tissue plasminogen activator treatment in experimental thromboembolic stroke. Stroke 34: 2019-2024.

27. Dwivedi A, Glynn A, Johnson S, Duffy S, Fereidoonnezhad B, et al. (2021) Measuring the effect of thrombosis, thrombus maturation and thrombolysis on clot mechanical properties in an in-vitro model. Journal of Biomechanics 129: 110731.

28. Duffy S, Farrell M, McArdle K, Thornton J, Vale D, Ret al. (2017) Novel methodology to replicate clot analogs with diverse composition in acute ischemic stroke. Journal of NeuroInterventional Surgery 9: 486-491.

29. Sorimachi T, Morita K, Ito Y, Fujii Y (2011) Blood pressure measurement in the artery proximal and distal to an intra-arterial embolus during thrombolytic therapy. Journal of NeuroInterventional Surgery 3: 43-46.

30. Desjardins J, Maillé JG, Lussier J, Grondin P (1979) A Simple Device for Achieving Pulsatile Flow During Cardiopulmonary Bypass. Annals of Thoracic Surgery 27: 178-180.

31. Hladovec J, Riba P (1975) The model of thrombosis and thrombolysis in vitro. Thrombosis Research 7: 743-752.

32. Meairs S, Dempfle CE, Pfaffenberger S, Speidl WS, Wojta J, et al. (2005) In vitro models for assessing transcranial ultrasound-enhanced thrombolysis [3] (multiple letters). Stroke 36: 929-931.

33. Yamashita D, Matsumoto Y, Tamaoki Y, Ueda Y, Okada H, et al. (2022) In vitro analysis of mechanism of pulsed-laser thrombolysis. PLOS ONE 17: e0262991.

34. Loyau S, Ho-Tin-noé B, Bourrienne MC, Boulaftali Y, Jandrot-Perrus M (2018) Microfluidic modeling of thrombolysis effect of antiplatelet and anticoagulant agents on tpa (tissue-type plasminogen activator)-induced fibrinolysis. Arteriosclerosis, Thrombosis, and Vascular Biology 38: 2626-2637.

35. Bannish BE, Chernysh IN, Keener JP, Fogelson AL, Weisel JW (2017a) Molecular and Physical Mechanisms of Fibrinolysis and Thrombolysis from Mathematical Modeling and Experiments. Scientific Reports 7: 1-11.

36. Piebalgs A, Gu B, Roi D, Lobotesis K, Thom S, et al. (2018) Computational Simulations of Thrombolytic Therapy in Acute Ischaemic Stroke. Scientific Reports 8: 15810.

37. Anand M, Rajagopal K, Rajagopal KR (2005) A Model for the Formation and Lysis of Blood Clots. Pathophysiology of Haemostasis and Thrombosis 34: 109-120.

38. Piebalgs A, Xu XY (2015) Towards a multi-physics modelling framework for thrombolysis under the influence of blood flow. Journal of The Royal Society Interface 12.

39. Bajd F, Serša I (2013) Mathematical Modeling of Blood Clot Fragmentation During Flow-Mediated Thrombolysis. Biophysical Journal 104: 1181-1190.

40. Farkas ÁZ, Farkas VJ, Szabó L, Wacha A, Bóta A, et al. (2019) Structure, Mechanical, and Lytic Stability of Fibrin and Plasma Coagulum Generated by Staphylocoagulase From Staphylococcus aureus. Frontiers in Immunology 10: 2967.

41. Rijken DC, Abdul S, Malfliet JJMC, Leebeek FWG, Uitte de Willige S (2016) Compaction of fibrin clots reveals the antifibrinolytic effect of factor XIII.

Journal of Thrombosis and Haemostasis 14: 1453-1461.

42. Tutwiler V, Peshkova AD, Le Minh G, Zaitsev S, Litvinov RI, et al. (2019) Blood clot contraction differentially modulates internal and external fibrinolysis. Journal of Thrombosis and Haemostasis 17: 361-370.

43. Tutwiler V, Singh J, Litvinov RI, Bassani JL, Purohit PK, et al. (2020) Rupture of blood clots: Mechanics and pathophysiology. Science Advances 6: eabc0496.

44. Johnson S, Chueh J, Gounis MJ, McCarthy R, Patrick McGarry J, et al. (2020) Mechanical behavior of in vitro blood clots and the implications for acute ischemic stroke treatment. Journal of NeuroInterventional Surgery 12: 853-857.

45. Bannish BE, Chernysh IN, Keener JP, Fogelson AL, Weisel JW (2017b) Molecular and Physical Mechanisms of Fibrinolysis and Thrombolysis from Mathematical Modeling and Experiments. Scientific Reports 7: 1-11.

46. Devcic-Kuhar B, Pfaffenberger S, Gherardini L, Mayer C, Gröschl M, et al. (2004) Ultrasound affects distribution of plasminogen and tissue-type plasminogen activator in whole blood clots in vitro. Thrombosis and Haemostasis 92: 980-985.

47. Diamond S (1999) Engineering design of optimal strategies for blood clot dissolution. Annual review of biomedical engineering 1: 427-461.

48. Mehta BP, Nogueira RG (2012) Should clot composition affect choice of Endovascular therapy? Neurology 79: s63–s67.

49. Anand S, Diamond S (1996) Computer Simulation of Systemic Circulation and Clot Lysis Dynamics During Thrombolytic Therapy That Accounts for Inner Clot Transport and Reaction. Circulation 94: 763-774.

50. Diamond S, Anand S (1993) Inner clot diffusion and permeation during fibrinolysis. Biophysical journal 65: 2622-2643.

51. Konduri PR, Marquering HA, van Bavel EE, Hoekstra A, Majoie CBLM (2020) In-Silico Trials for Treatment of Acute Ischemic Stroke. Frontiers in Neurology 11: 558125.

52. Luraghi G, Matas JFR, Dubini G, Berti F, Bridio S, et al. (2021) Applicability assessment of a stent-retriever thrombectomy finite-element model. Interface Focus 11: 20190123.

Citation: Dwivedi A, Burke J, Mirza M, Gilvarry M, Dwivedi A (2023) Introducing a Novel *in-vitro* Model of Thrombolysis in Acute Ischemic Stroke. J Biomed Res Rev Vol: 6, Issu: 1. (01-11).